Journal of Thermal Science Vol.27, No.4 (2018) 321−330

https://doi.org/10.1007/s11630-018-1019-y **Article ID: 1003-2169(2018)04-0321-10**

Optimization of Dimples in Microchannel Heat Sink with Impinging Jets—Part B: the Influences of Dimple Height and Arrangement

MING Tingzhen[1,2*], CAI Cunjin[1], YANG Wei[3], SHEN Wenqing[4], FENG Wei[2], ZHOU Nan[2]

1. School of Civil Engineering and Architecture, Wuhan University of Technology, No.122, Luoshi Road, Wuhan 430070, China
2. China Energy Group, Environmental Energy Technologies Division, Lawrence Berkeley National Laboratory, 1 Cyclotron Road, Berkeley, CA 94720 USA
3. Hubei Institute of Aerospace Chemical Technology, Xiangyang 441000, China
4. G. W. Woodruff School of Mechanical Engineering, Georgia Institute of Technology, Atlanta, 30332 USA

Abstract: The combination of a microchannel heat sink with impinging jets and dimples (MHSIJD) can effectively improve the flow and heat transfer performance on the cooling surface of electronic devices with very high heat fluxes. Based on the previous work by analysing the effect of dimple radius on the overall performance of MHSIJD, the effects of dimple height and arrangement were numerically analysed. The velocity distribution, pressure drop, and thermal performance of MHSIJD under various dimple heights and arrangements were presented. The results showed that: MHSIJD with higher dimples had better overall performance with dimple radius being fixed; creating a mismatch between the impinging hole and dimple can solve the issue caused by the drift phenomenon; the mismatch between the impinging hole and dimple did not exhibit better overall performance than a well-matched design.

Keywords: microchannel with impinging jets and dimples, impinging jet, dimple, heat transfer enhancement, thermal resistance

1. Introduction

Heat transfer enhancement is always a hot spot in many research fields and industrial applications, such as energy, power plant, metallurgy, chemical engineering, aerospace, building and environment, human thermal comfort, and so on. There are two research branches of heat transfer enhancement: fundamental theories and technical improvement. The field synergy principle [1-4] and the theory of entropy generation extremum and entransy dissipation extremum for heat transfer optimization [5] are the most widely accepted fundamental theories since the beginning of the 21st century. Whereas technical improvement mainly concerning the methods used in various scenarios with heat exchange, such as power stations [6], power battery [7], hypersonic heating structure [8], porous media [9-11], phase-change heat transfer [12] and electronic devices [13].

Received: May 08, 2018 Corresponding author: MING Tingzhen, Professor E-mail: tzming@whut.edu.cn
This study is financially supported by the National Natural Science Foundation of China (Grant No. 51778511), the Hubei Provincial Natural Science Foundation of China (Grant No. 2018CFA029), and the Key Project of ESI Discipline Development of Wuhan University of Technology (WUT Grant No. 2017001)

For the thermal management of semiconductor industry, the heat flux density of electronic devices increases greatly to about 500 W/cm^2 [13]. Existing single method, such as microchannel heat transfer [14], impinging jets [15], fins [16], and dimples [17], is difficult to effectively remove the waste heat away from the chips of electronic devices with very high heat fluxes. Therefore, the combination of several technologies can be one of the solutions [18, 19].

Earlier research showed that, by combining a microchannel and impinging jets, better heat exchange performance could be achieved compared with the application of an individual cooling technology [20, 21]. Further, a very interesting finding having been verified by several researchers is that: appropriate design of dimples will achieve less flow resistance [13, 22].

Based on the previous research by Huang et al. [13] and Ming et al. [22], a heat transfer element with the combination of a microchannel, impinging jets, and dimpled surface was considered; a comprehensive mathematical model describing the flow and heat transfer characteristics was advanced; and the effect of dimple radius on the overall performance was analyzed. However, the effects of dimple height and arrangement on the heat transfer element's flow and heat transfer performances have not yet been considered. The present study will further implement the dimple optimization in microchannel heat sink with impinging jets and dimples (MHSIJD). We will use numerical simulation to analyze the effects of the height and arrangement of the dimples on the flow and heat transfer performance of MHSIJD.

2. Physical and mathematical model

Fig. 1 illustrates the microchannel heat sink with impinging jets and dimples (MHSIJD) [22]. Two sets of 12 impinging holes were uniformly distributed on the microchannel ceiling with outlets facing the dimples. The heat sink at the bottom conducted heat from the chip to the microchannel. Water was the working fluid, injected through impinging holes. Fig. 1(a) shows the entire model. Considering the symmetry of the microchannel with impinging jet along the X and Y axes, we simulated 1/8 of the model, as shown in Fig. 1(b).

In the computational model, L, W and H represent length, width, and height, respectively; the impinging hole is square with side length L_1 and height H_1; the spacing between impinging holes is L_2; the microchannel width is $2W_1$; and the height is H_2. Fig. 1(c) shows the symmetry plane; the dimple radius is r, and the height is *h′*. All geometric parameters are listed in Table 1, with dimple dimensions being listed in next section.

Mathematical model, boundary conditions, and numerical simulation procedure are clearly presented in previous study [22]. This work will mainly focus on the simulation results of the optimization of dimples.

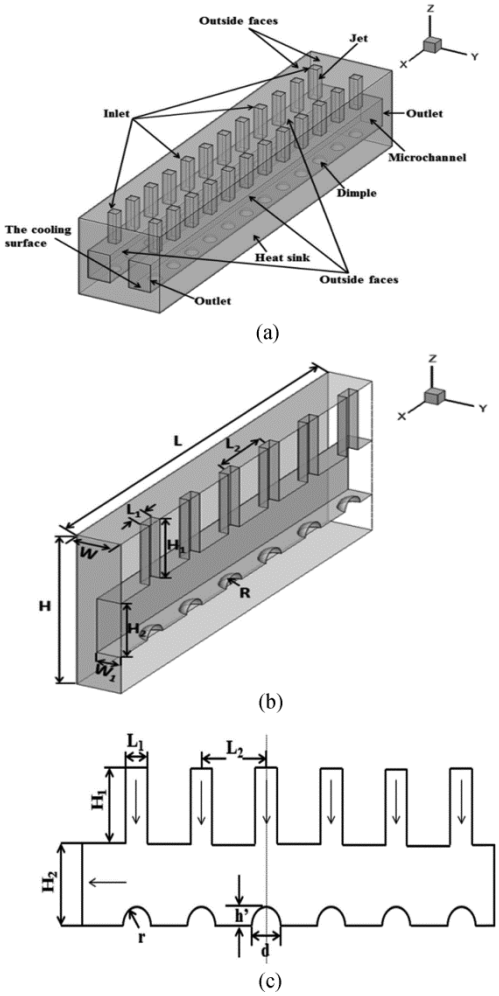

Fig. 1 MHSIJD: (a) overall MHSIJD model with dimples; (b) computational domain; (c) part of the symmetry plane [22]

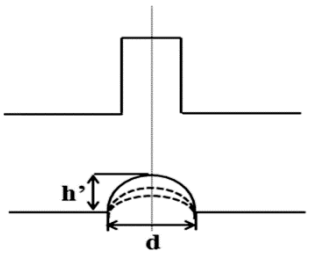

Fig. 2 Dimple design of different heights and fixed projection radii

Table 1 Geometric parameters of MHSIJD [22]

L/mm	W/mm	H/mm	L_1/mm
9.100	0.920	4.150	0.390
H_1/mm	L_2/mm	W_1/mm	H_2/mm
1.650	1.430	0.500	1.500

3. Simulation results and analysis

3.1 The effect of dimple height

To study the effect of dimple height, we altered the height while fixing the projection radius of the dimple on the cooling surface at 0.275 mm. Four different h'/d ratios were compared. As shown in Fig. 2, the dimple center was aligned with the jet nozzle.

3.1.1 Effect of dimple height on heat transfer

The heat flux density of the heated wall was 500W/cm^2. Figs. 3(a) and (b) show temperature distribution at the MHSIJD symmetry plane with different dimple heights when the total mass flow rates were 2 g/s and 30 g/s, respectively. In sets (a) and (b), the temperature boundary layer was thicker with smaller mass flow. For h'/d between 0.25 and 0.5 with m = 2 g/s, no obvious change in maximum temperature appeared in the system; h'/d = 0.2 resulted in a much lower maximum temperature than that in other cases. For set (b), we observed no major change in maximum temperature because the mass flow rate was sufficiently large and had strong cooling power for different positions.

Fig. 4 shows the velocity distribution at the symmetry MHSIJD plane with different dimple heights. Influenced by the flow from upstream, the impinging jets near the outlet failed to have direct heat change with the cooling surface, called the drift phenomenon [13]. The drift phenomenon seriously weakens the impact of impinging jets. Comparing the exit location of the rightmost jet in set (b), the drift phenomenon was more obvious in the design with lower dimples.

Fig. 5 plots the average temperature of the cooling surface versus dimple height. The larger the mass flow rate, the lower the temperature at the cooling surface. When the mass flow rate was sufficient, the average temperature converged gradually. Comparing different lines in the figure, a higher dimple generally resulted in a lower average temperature, presumably because a higher dimple has a larger surface, and dimples can disturb the flow near the fluid-solid interface. A higher dimple caused stronger disturbance, which facilitated heat exchange.

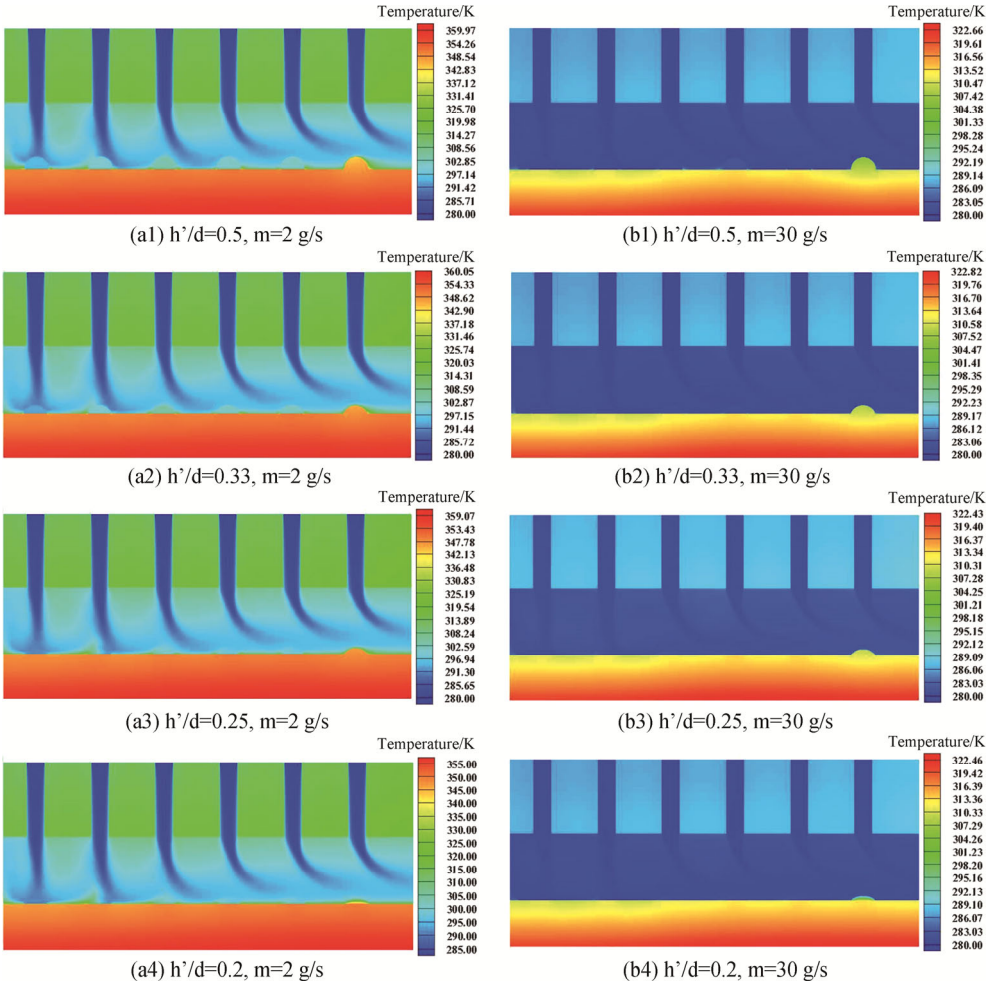

Fig. 3 Temperature distribution at the MHSIJD symmetry plane with different dimple heights

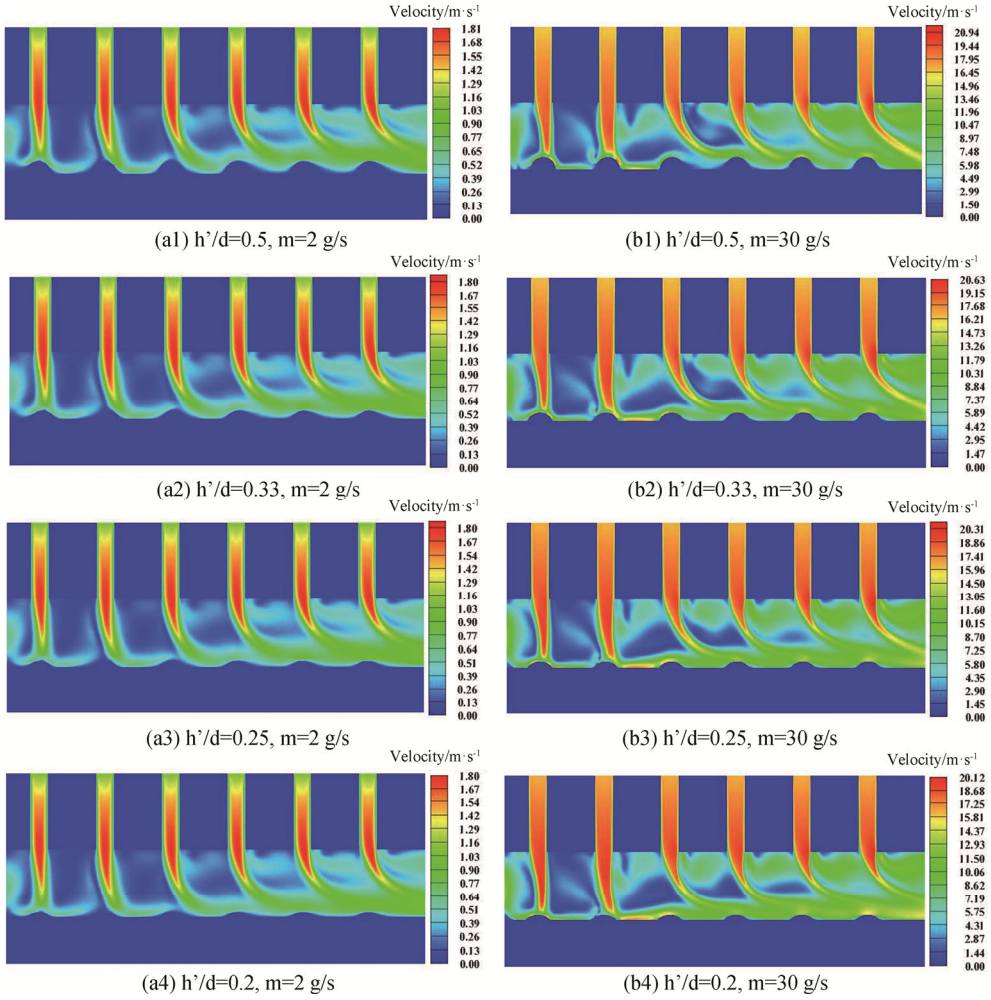

Fig. 4 Velocity distribution at the MHSIJD symmetry plane with different dimple heights

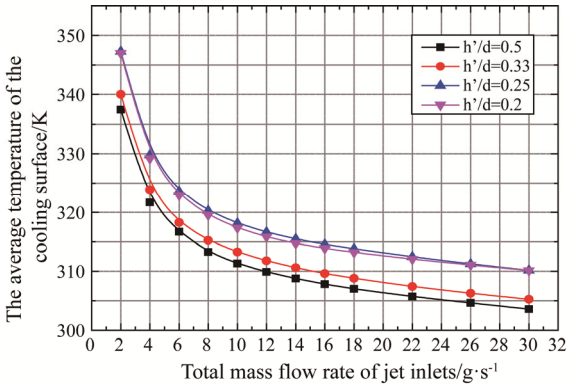

Fig. 5 Average temperature of the cooling surface in designs with different dimple heights

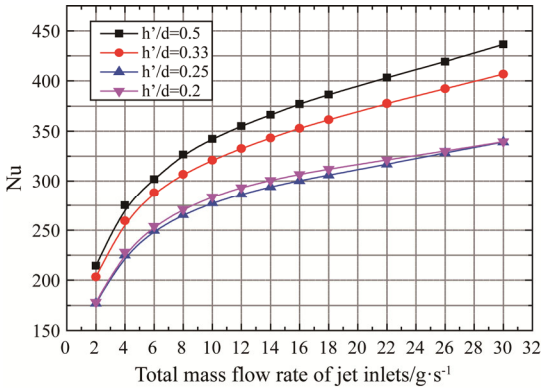

Fig. 6 Nusselt number of the cooling surface of designs with different dimple heights

Fig. 6 shows the Nusselt number (Nu) of the cooling surface in designs with different dimple heights. Like the analysis in the previous section, the trend of Nu was found to be inverse to that of the average temperature at the cooling surface.

3.1.2 Effect of dimple height on flow resistance

Fig. 7 shows the pressure distribution at the MHSIJD symmetry plane with different dimple heights. In set (a), the maximum pressure decreased with decreasing dimple height; in set (b), the maximum pressure decreased first

and then increased with decreasing dimple height.

The pressure drop of MHSIJD with different dimple heights is shown in Fig. 8. When the mass flow rate was small, the height of the dimple had a negligible effect on the pressure drop. When the mass flow rate was large, lower dimples resulted in a higher pressure drop. Higher dimples demonstrated better flow guidance for impinging jets.

3.1.3 Effect of dimple height on overall performance

Fig. 9 shows the overall performance of MHSIJD with different dimple heights. A larger h'/d generally led to better overall performance. For different dimple heights, the heat transfer coefficient was highly varied, although we noted no significant change in pressure drop. Thus, the overall performance essentially followed the trend of

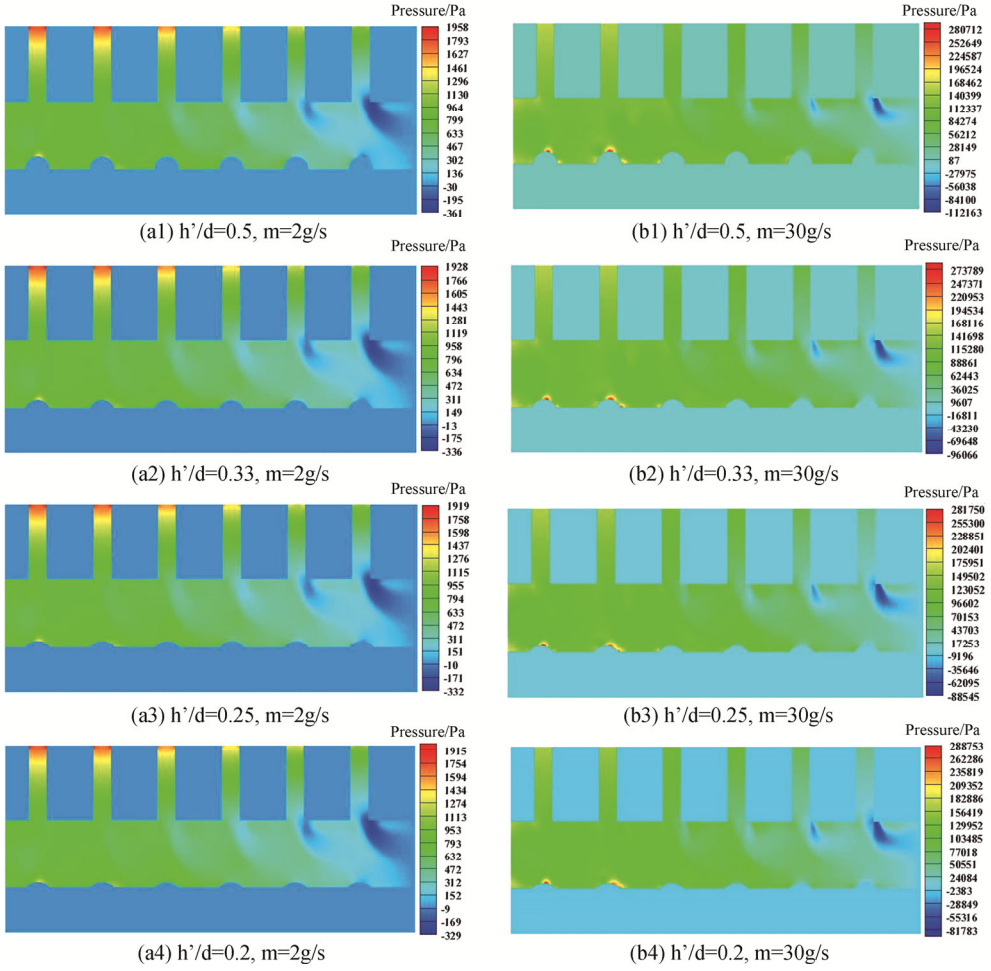

Fig. 7 Pressure distribution at the MHSIJD symmetry plane with different dimple heights

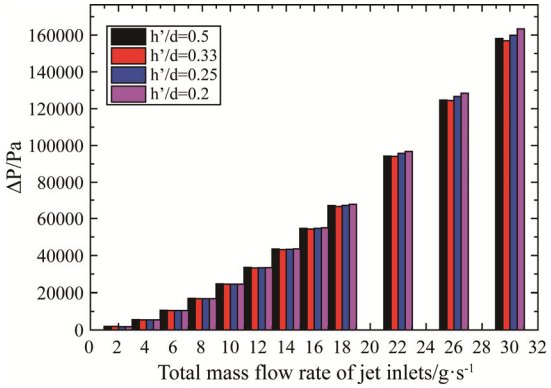

Fig. 8 Pressure drop of MHSIJD with different dimple heights

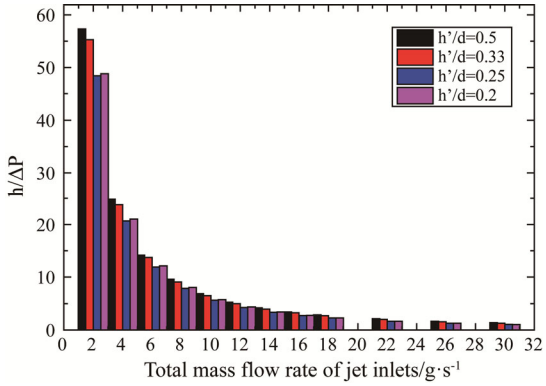

Fig. 9 Overall performance of MHSIJD with different dimple heights

the heat transfer coefficient. A large mass flow rate and high dimples achieved optimal overall performance.

3.2 The effect of dimple

In this section, the radius of the dimple was fixed at 0.195 mm, and the dimple was semi-spherical. Instead of aligning the center of the impinging hole and the dimple, dimples could be placed with some bias. We shifted all dimples rightwards with different levels. As shown in Fig.10, the distance between the center of the impinging hole and the center of the dimple in the horizontal plane ranged from 0 to L.

3.2.1 Effect of dimple location on heat transfer

The heat flux density at the heated surface was fixed at 500 W/cm^2 for all cases. Fig. 11 shows the temperature distribution of MHSIJD with different dimple arrangements. For a small mass flow rate, with $\Delta L = 0$, only the first jet impinged directly on the dimple; the other jets could not directly cool the corresponding dimple. When $\Delta L > 0$, the first jet might impinge on the dimple edge, but the remaining jets could impinge on the corresponding dimples. When only considering the benefit of the jets impinging on the dimples, there is a tradeoff when choosing the ΔL value. A large ΔL could strengthen cool-

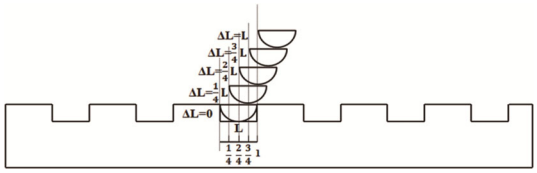

Fig. 10 Different dimple locations in correspondence to impinging hole (aerial view)

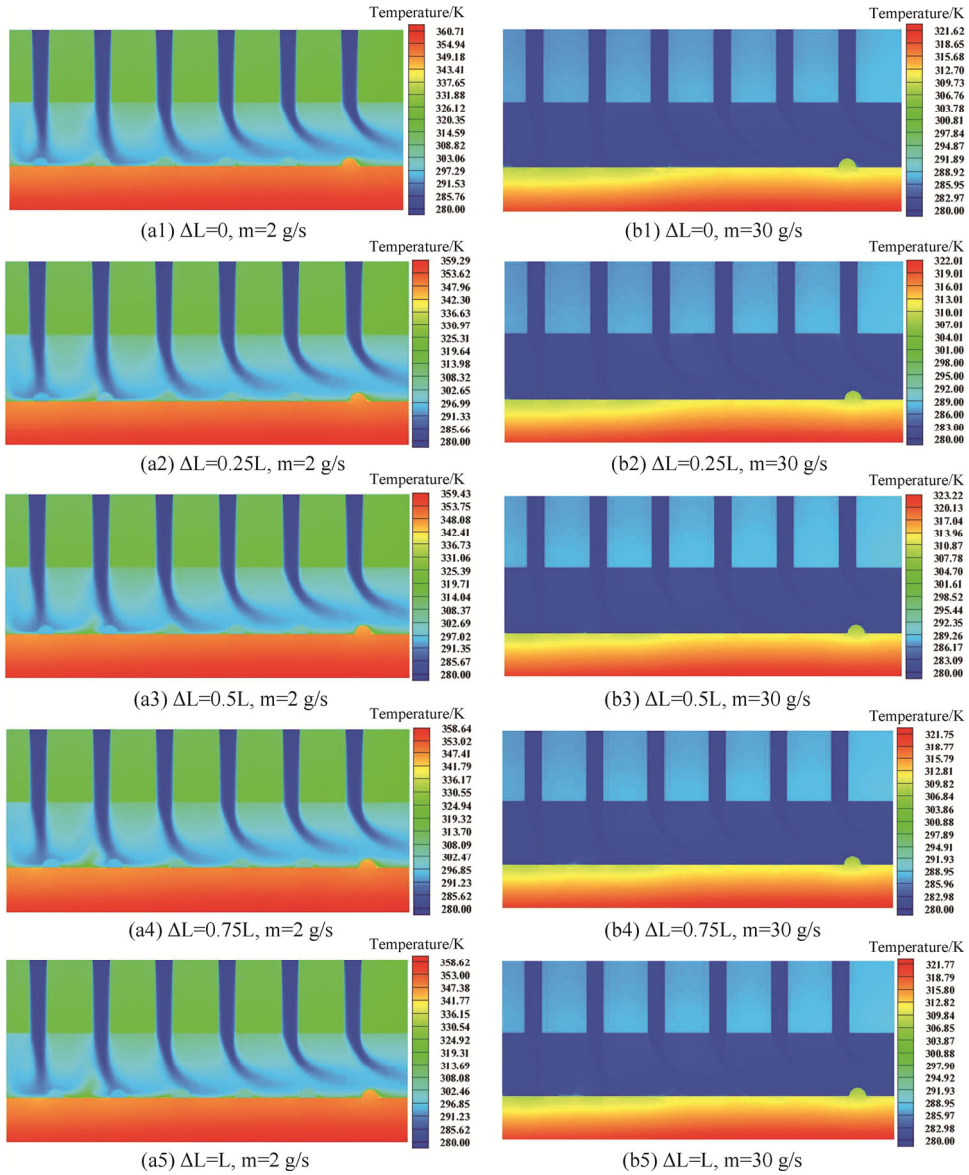

Fig. 11 The temperature distribution at MHSIJD symmetry plane with different dimple arrangements

ing downstream but weaken cooling upstream. For a small flow rate, the maximum temperature decreased with increasing ΔL; for a large flow rate, the maximum temperature first increased and then decreased with increasing ΔL.

Fig. 12 shows the velocity distribution of MHSIJD with different dimple arrangements. The drift phenomenon [13] was pronounced in each case. If the cool water from the impinging jet could not reach the cooling surface, the fluid on the surface moved from upstream and had a higher temperature than the impinging jet. Also, the velocity near the surface was mainly controlled by the upstream. With warmer fluid and slower flow at the downstream surface, heat exchange was less efficient for downstream than upstream. In graphs (b1)–(b5), comparing the length of the jet core with high velocity downstream, with an increase in ΔL, the drift phenomenon became more obvious initially and then became less obvious. This trend aligned well with the maximum system temperature, as shown in Fig. 11. The effect of ΔL was not readily apparent for a small mass flow rate.

Fig. 13 shows the average temperature of the cooling surface with different dimple arrangements. For certain mass flow rates, the average temperature of the cooling surface increased first and then decreased with increasing ΔL · ΔL = 0.5L was the worst case among all tested designs, whereas ΔL = 0 was the best case. The trend was quite similar to that of the maximum temperature in the whole system for the same reason as explained in the prior section. The Nu number of each case is shown in Fig. 14. Similar to previous analysis, the Nu had an inverse trend of average temperature at the cooling surface.

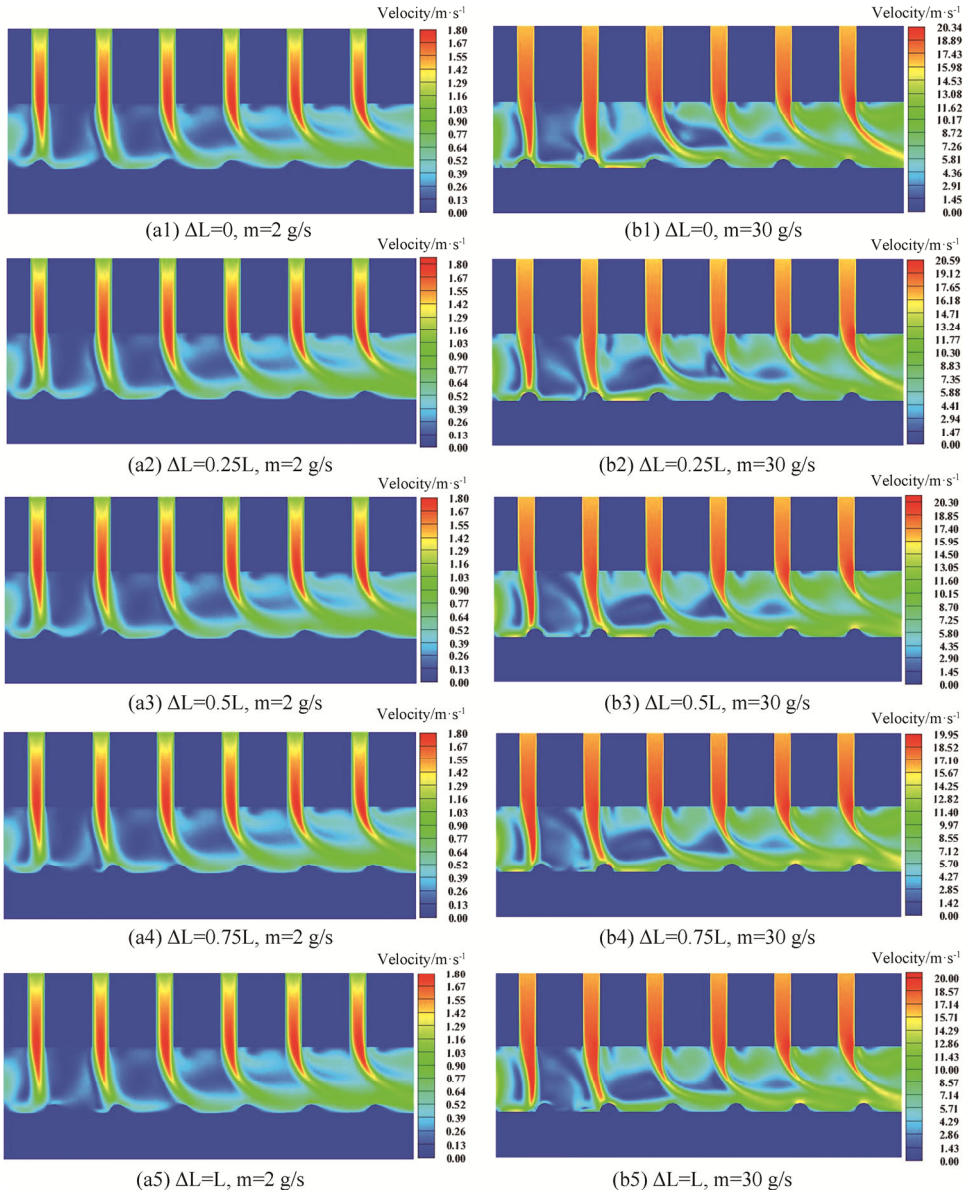

Fig. 12 Velocity distribution at MHSIJD symmetry plane with different dimple arrangements

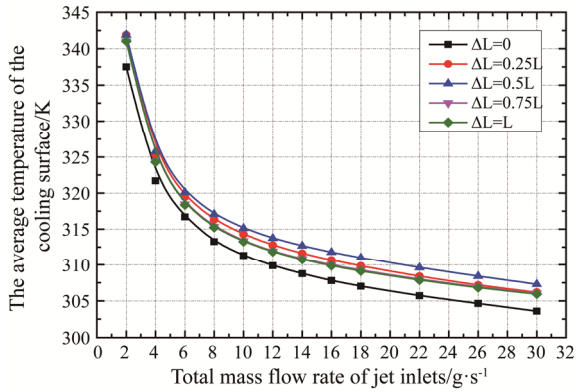

Fig. 13 Average temperature of the cooling surface of MHSIJD with different dimple arrangements

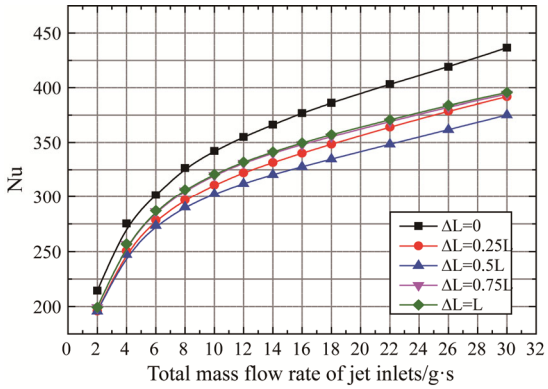

Fig. 14 Nusselt number of the cooling surface of MHSIJD with different dimple arrangements

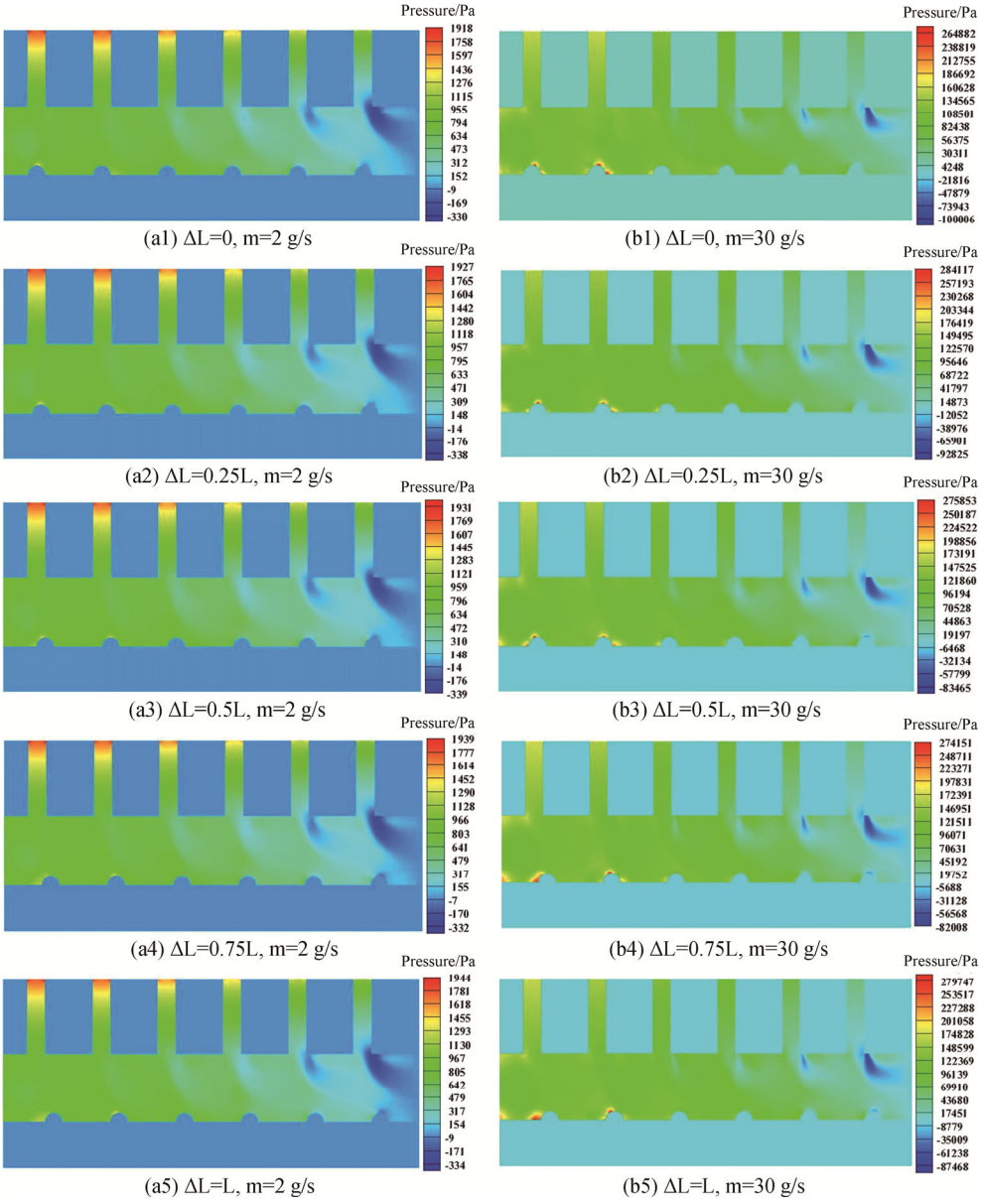

Fig. 15 Pressure distribution at MHSIJD symmetry plane with different dimple arrangements

3.2.2 Effect of dimple arrangement on flow resistance

Fig. 15 shows the pressure distribution at the MHSIJD symmetry plane with different dimple arrangements. For a small flow rate, the maximum pressure was at the inlet of the first jet; for a large flow rate, it was at the upstream dimples. Fig. 16 shows the pressure drop in dimple cases. When the mass flow rate was low, the pressure drop was similar for different designs. With a large mass flow rate, the pressure drop increased with ΔL. Upstream, larger ΔL led to greater bias between the impinging jet and dimple center. The dimple structure guided the impinging jet and decreased the pressure drop. Though the change of ΔL could also affect the pressure drop downstream, the effect was not that important due to the drift phenomenon; therefore, a large ΔL resulted in greater power assumption.

3.2.3 Effect of dimple arrangement on overall performance

The overall performance of MHSIJD with different dimple arrangements is presented in Fig. 17. At a certain mass flow rate, the overall performance was worst at $\Delta L = 0.5L$ and best at $\Delta L = 0$. These results follow the average temperature trend of the cooling surface, but not that of a pressure drop. Without considering temperature uniformity at the cooling surface, according to the analyzed cases, it would be better to align the dimple center with the impinging jet (i.e., $\Delta L = 0$).

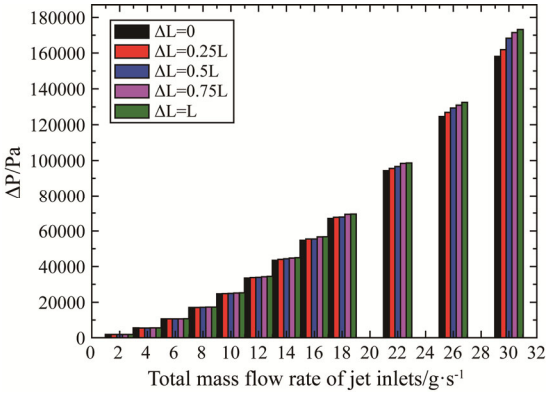

Fig. 16 Pressure drop of MHSIJD with different dimple arrangements

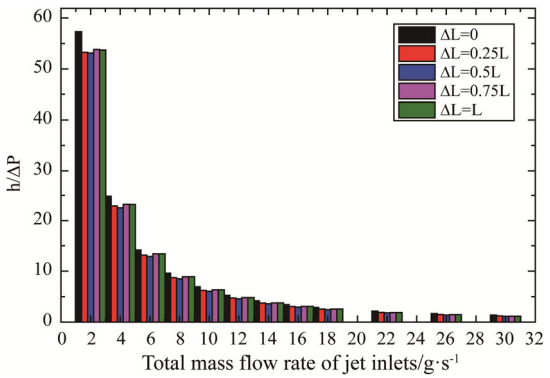

Fig. 17 Overall performance of MHSIJD with different dimple arrangements

4. Conclusions

In this paper, the dimple parameters including dimple height and location were optimized via numerical simulation. From the results, the following conclusions can be drawn:

(1) When the dimple radius was fixed, higher dimples generally resulted in higher heat transfer coefficients and lower pressure drops; therefore, MHSIJD with higher dimples had better overall performance.

(2) Creating a mismatch between the impinging hole and dimple can solve the issue caused by the drift phenomenon. The bias ΔL between the impinging hole and the dimple center showed different effects for upstream and downstream. The heat transfer coefficient decreased first and then increased with ΔL. Although larger ΔL led to higher pressure drops, the change in pressure drop was not enormously important, and the overall performance demonstrated the same trend as the heat transfer coefficients.

In summary, optimal cooling performance can be achieved with large and high dimples. Among tested designs, the mismatch between the impinging hole and dimple did not exhibit better overall performance than a well-matched design.

References

[1] Guo Z.Y., Li D.Y., Wang B.X.. A novel concept for convective heat transfer enhancement. International Journal of Heat and Mass Transfer. 1998, 41(14): 2221–2225.

[2] Liu W., Liu Z.C., Ma L. Application of a multi-field synergy principle in the performance evaluation of convective heat transfer enhancement in a tube. Science Bulletin. 2012, 57(13): 1600–1607.

[3] Wei L., Liu Z.C., Guo Z.Y. Physical quantity synergy in laminar flow field of convective heat transfer and analysis of heat transfer enhancement. Science Bulletin. 2009, 54(19): 3579–3586.

[4] Guo Z.Y., Tao W.Q., Shah R. The field synergy (coordination) principle and its applications in enhancing single phase convective heat transfer. International Journal of Heat and Mass Transfer. 2005. 48(9): 1797–1807.

[5] Liu X., Meng J., Guo Z. Entropy generation extremum and entransy dissipation extremum for heat exchanger optimization. Chinese Science Bulletin. 2009, 54(6): 943–947.

[6] Szwaba R., Kaczynski P., Telega J., Doerffer P. Influence

of internal channel geometry of gas turbine blade on flow structure and heat transfer. Journal of Thermal Science. 2017, 26(6): 514–522.

[7] An Z., Jia L., Ding Y., Dang C., Li X. A review on lithium-ion power battery thermal management technologies and thermal safety. Journal of Thermal Science. 2017, 26(5): 391–412.

[8] Qin J., Ning D., Feng Y., Zhang J., Feng S., Bao W. A new method of thermal protection by opposing jet for a hypersonic aeroheating strut. Journal of Thermal Science. 2017, 26(3): 282–288.

[9] Guo C., Nian X., Liu Y., Qi C., Song J., Yu W. Analysis of 2D flow and heat transfer modeling in fracture of porous media. Journal of Thermal Science. 2017, 26(4): 331–338.

[10] Huang Z.F., Nakayama A., Yang K., Yang C., Liu W. Enhancing heat transfer in the core flow by using porous medium insert in a tube. International Journal of Heat and Mass Transfer. 2010, 53(5–6): 1164–1174.

[11] Yu B.M., Liu W. Fractal analysis of permeabilities for porous media. AIChE Journal. 2004, 50(1): 46–57.

[12] Quan X., Cheng P., Wu H. An experimental investigation on pressure drop of steam condensing in silicon microchannels. International Journal of Heat & Mass Transfer. 2008, 51(21): 5454–5458.

[13] Huang X., Yang W., Ming T., Shen W., Yu X. Heat transfer enhancement on a microchannel heat sink with impinging jets and dimples. International Journal of Heat and Mass Transfer. 2017, 112: 113–124.

[14] Wang G., Cheng P., Bergles A.E. Effects of inlet/outlet configurations on flow boiling instability in parallel microchannels. International Journal of Heat & Mass Transfer. 2008, 51(9-10): 2267–2281.

[15] Cooper D., Jackson D., Launder B., Liao G. Impinging jet studies for turbulence model assessment-- Ⅰ. Flow-field experiments. International Journal of Heat & Mass Transfer. 1993, 36(10): 2675–2684.

[16] Lee Y.J., Lee P.S., Chou S.K. Enhanced microchannel heat sinks using oblique fins. Conference Enhanced microchannel heat sinks using oblique fins. p. 253–260.

[17] Chang S.W., Chiang K.F., Chou T.C. Heat transfer and pressure drop in hexagonal ducts with surface dimples. Experimental Thermal & Fluid Science. 2010, 34(8): 1172–1181.

[18] Ming T.Z., Ding Y., Gui J.L., Tao Y.X. Transient thermal behavior of a microchannel heat sink with multiple impinging jets. Journal of Zhejiang University-SCIENCE A (Applied Physics & Engineering). 2015, 16(11): 894–909.

[19] Ming T.Z., Gui J.L., Peng C., Tao Y. Analysis of the hydraulic and thermal performances of a microchannel heat sink with extended-nozzle impinging jets. Heat Transfer Research. 2017, 48(10): 893–914.

[20] Seyf H.R., Zhou Z., Ma H.B., Zhang Y. Three dimensional numerical study of heat-transfer enhancement by nano-encapsulated phase change material slurry in microtube heat sinks with tangential impingement. International Journal of Heat & Mass Transfer. 2013, 56(1–2): 561–573.

[21] Zhuang Y., Ma C.F., Qin M. Experimental study on local heat transfer with liquid impingement flow in two-dimensional micro-channels. International Journal of Heat & Mass Transfer. 1997, 40(97): 4055–4059.

[22] Ming T., Cai C., Yang W., Shen W., Gan T. Optimization of dimples in microchannel heat sink with impinging jets —Part A: mathematical model and the influence of dimple radius. Journal of Thermal Science. 2018, 27(3): 195–202.